

Supplementary Information

Nitrogen-doped Carbon dots for the Sensitive Detection of Ferric Ions and Monohydrogen Phosphate by Naked Eye and Imaging in Living Cells

Qiaoling Liu,* Borong Ren, Kaixin Xie, Yanmei Yan, Ruirong, Liu, Shiyu Lv, Qing He, Boru Yang, Lin Li*

Department of Chemistry, Taiyuan Normal University, Jinzhong 030619, P. R. China.

*E-mail: liuqiaoling@tynu.edu.cn, Tel: +86-351-2886580;

*E-mail: lilin@tynu.edu.cn. Tel: +86-351-2886580

Contents

1. Determination of fluorescence quantum yield
2. Supplementary Figures and Table S1 and Table S2.
3. References

1. Determination of fluorescence quantum yield

Fluorescence quantum yield was measured by a standard method in air-equilibrated sample at room temperature. The fluorescence quantum yield was determined by using Rhodamine B ($\Phi=0.31$ in water) as reference.^{1, 2}

$$\Phi_{sam} = \Phi_{ref} \frac{I_{sam}}{I_{ref}} \cdot \frac{A_{ref}}{A_{sam}} \cdot \left(\frac{n_{sam}}{n_{ref}}\right)^2 \quad (1)$$

Where Φ is the fluorescence quantum yield, I is the integrated emission intensity, A is the absorbance, and n is the refractive index. The subscripts $_{sam}$ and $_{ref}$ stand for sample and reference, respectively. Herein, the N-CDs and Rhodamine B were dissolved in ultrapure water ($n = 1.33$) and excited under 420 nm and kept the absorbance below 0.05.

2. Supplementary figures

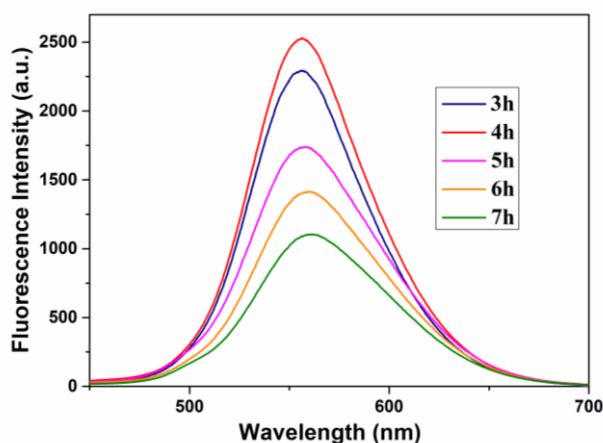


Fig.S1 Fluorescence emission spectra of the N-CDs based on o-phenylenediamine and formamide as the precursors with the mole ratio 1:1.5 at 150 °C for the different reaction times.

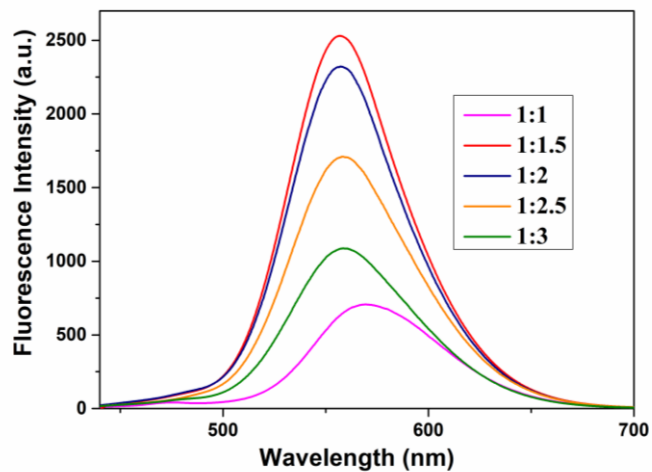


Fig.S2 Fluorescence emission spectra of the N-CDs based on o-phenylenediamine and formamide as the precursors at 150 °C for 4h with the different mole ratios between o-phenylenediamine and formamide.

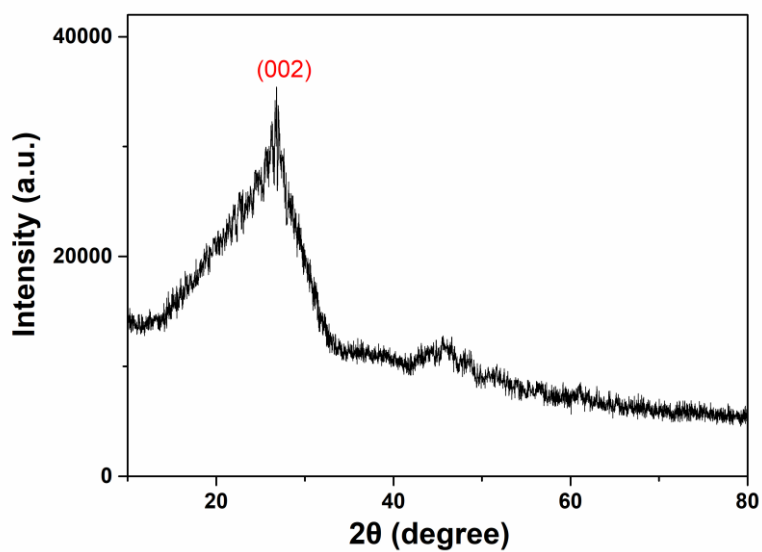


Fig.S3 XRD diffraction pattern of the N-CDs.

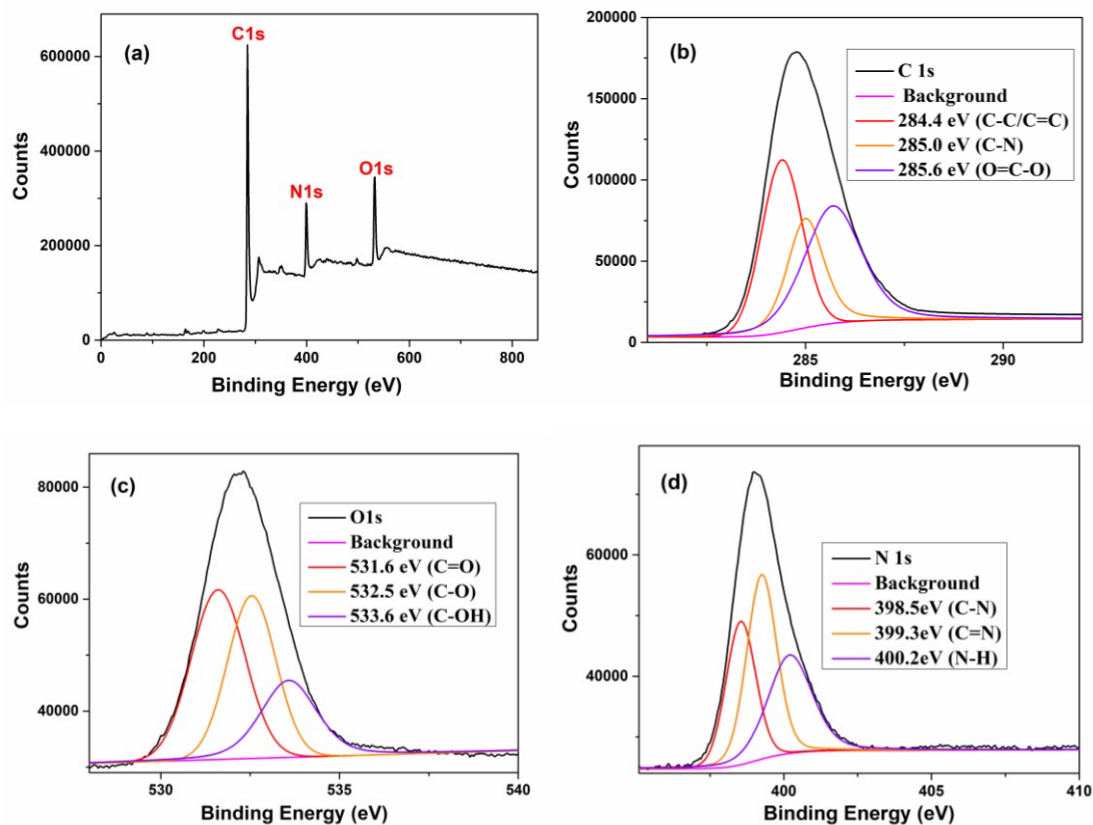


Fig.S4 (a) The full scan XPS of the N-CDs. High resolution XPS of C 1s (b), O 1s (c) and N 1s (d).

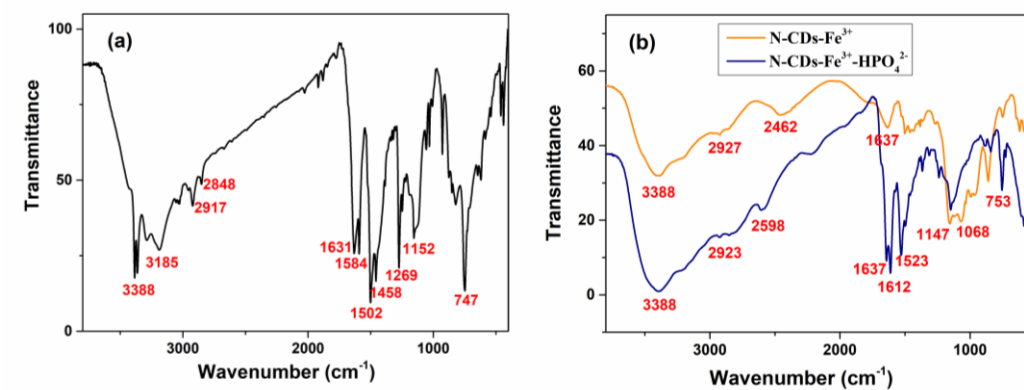


Fig.S5 Fourier transformed infrared spectra of the N-CDs (a) and the complexes of the N-CD-Fe³⁺ and the [N-CD-Fe³⁺-HPO₄²⁻] (b).

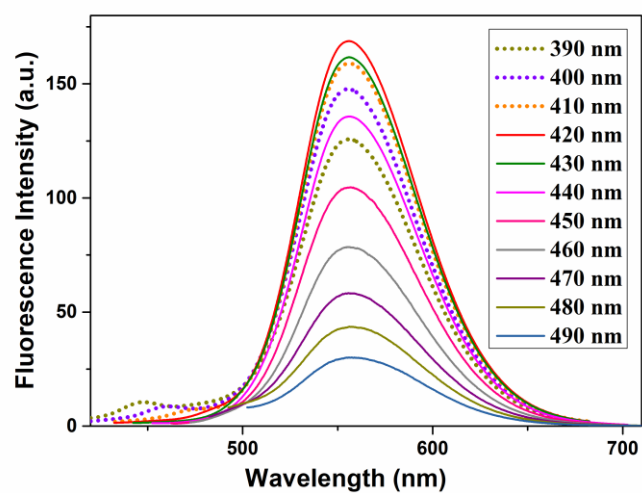


Fig.S6 The fluorescence emission spectra of the N-CDs at different excitation wavelengths.

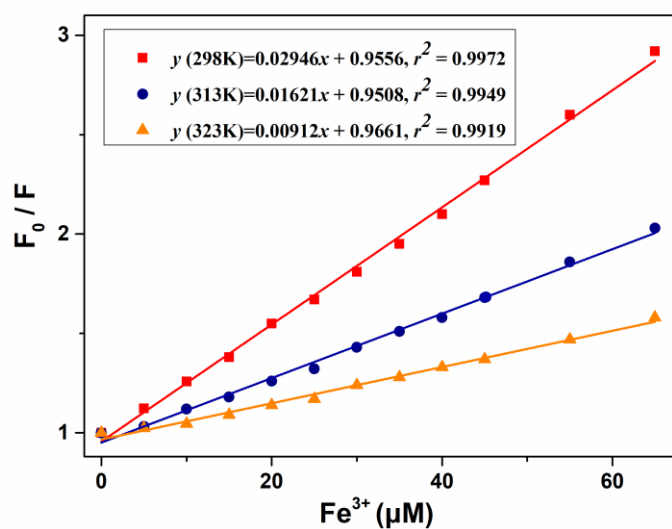


Fig.S7 Stern-Volmer plot at different temperatures (298 K, 318 K and 323K) and different concentrations of Fe^{3+} (0.3–65.0 μM).

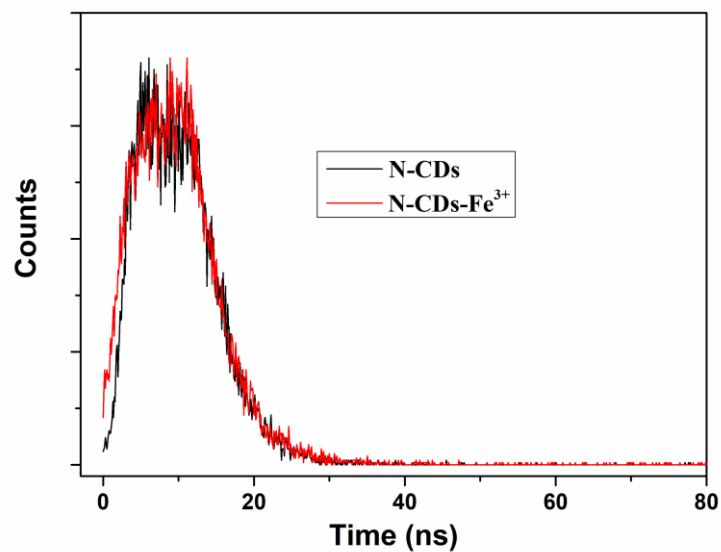


Fig.S8 Fluorescence lifetime decays of the N-CDs in the absence (black line) and presence (red line) of Fe³⁺ under excitation of 450 nm.

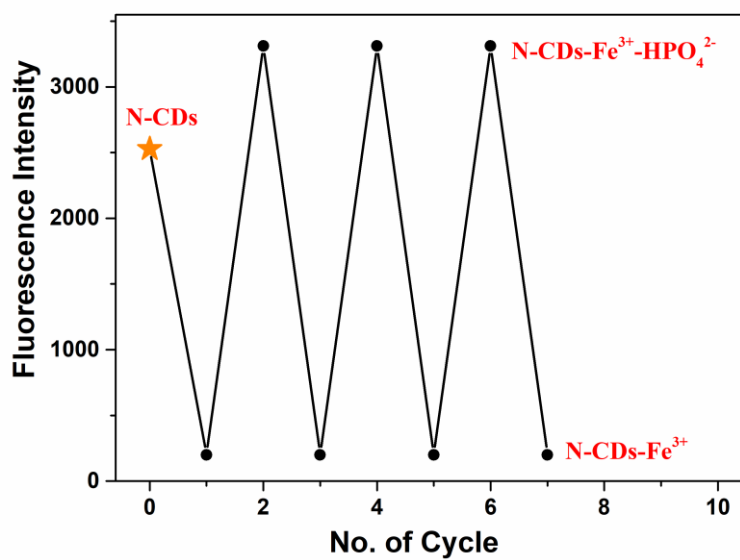


Fig.S9 Reversible fluorescence responses between N-CDs-Fe³⁺ and HPO₄²⁻ at 556 nm.

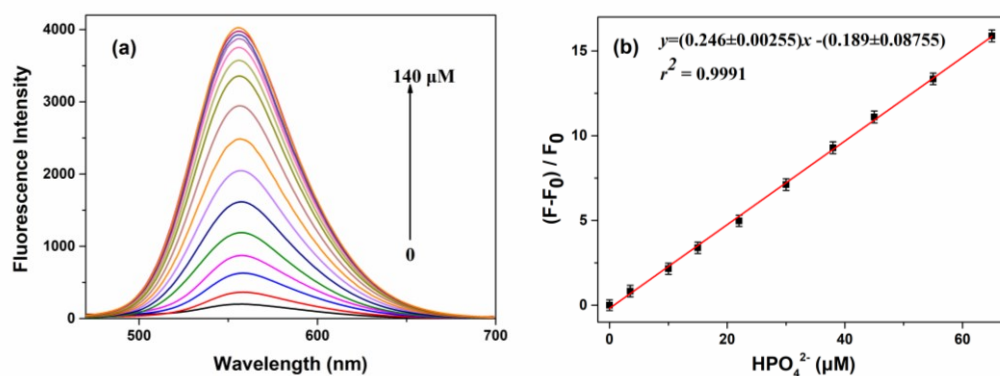


Fig.S10 (a) Fluorescence emission spectra of the N-CDs-Fe³⁺ complex in the presence of different concentrations of HPO₄²⁻ (0-140 μM). (b) Linear relationship between $[(F-F_0)/F_0]$ and the concentration of HPO₄²⁻, where F_0 and F are the fluorescence intensities of the N-CDs-Fe³⁺ complex at 556 nm in the absence and presence of HPO₄²⁻, respectively. The excitation wavelength is 415 nm.

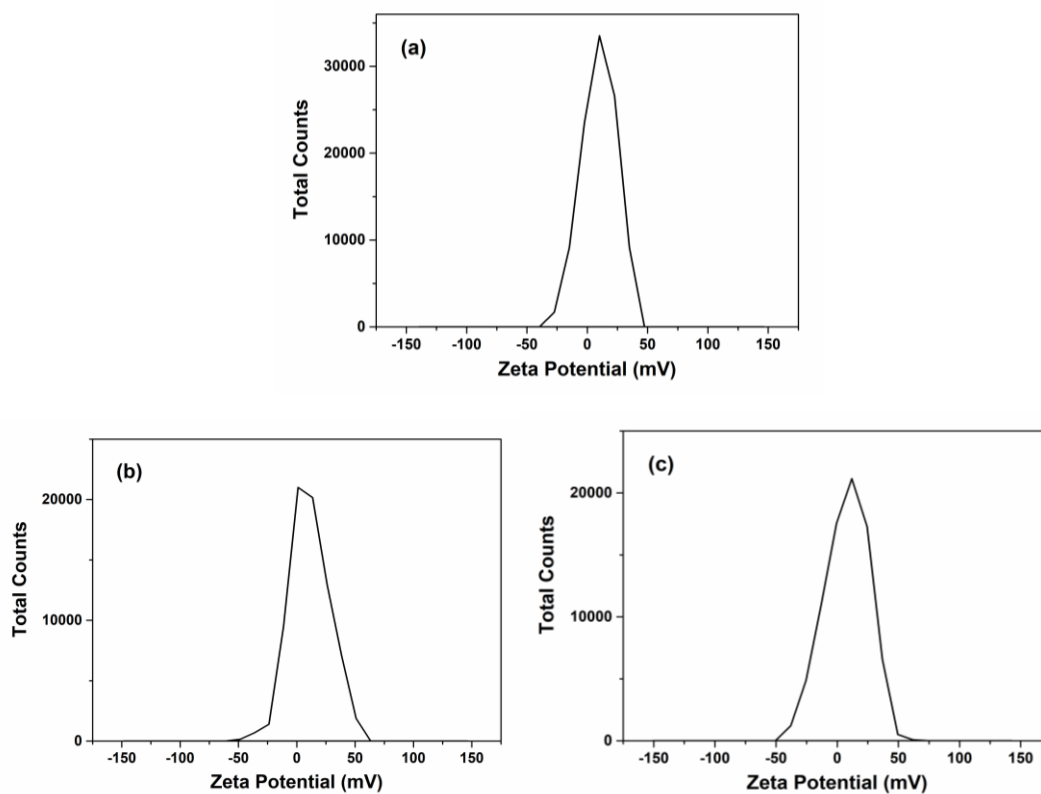


Fig.S11 Zeta potential plots of the N-CDs (a), the complexes of the N-CDs-Fe³⁺ (b) and the [N-CDs-Fe³⁺-HPO₄²⁻] (c).

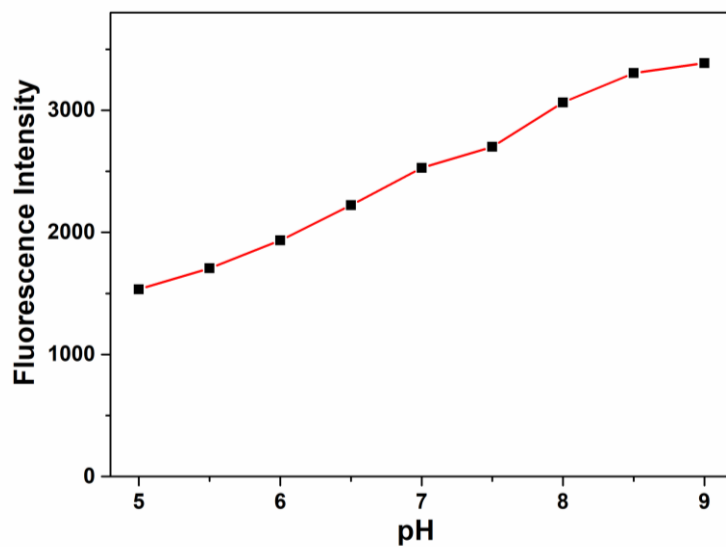


Fig.S12 Effect studies of pH on the fluorescence intensities of the N-CDs (0.04 mg/mL) at 556 nm.

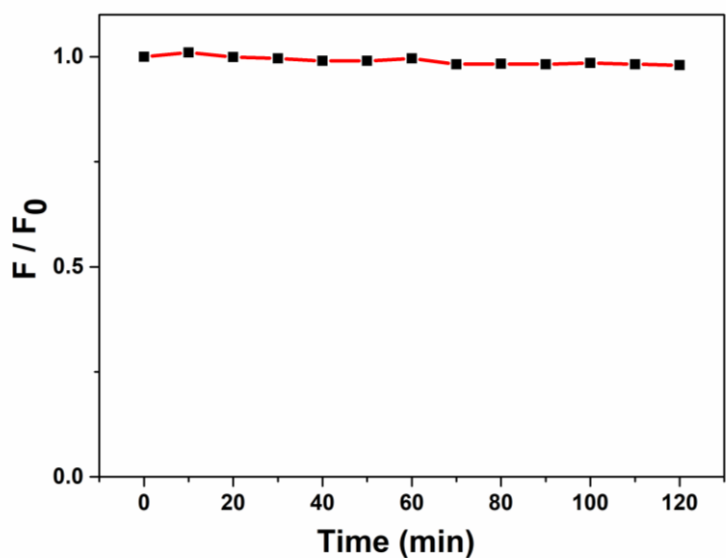


Fig.S13 Photostability studies of the N-CDs as a function of the continuous ultraviolet light at 365 nm for 120 min at 420 nm excitation wavelength.

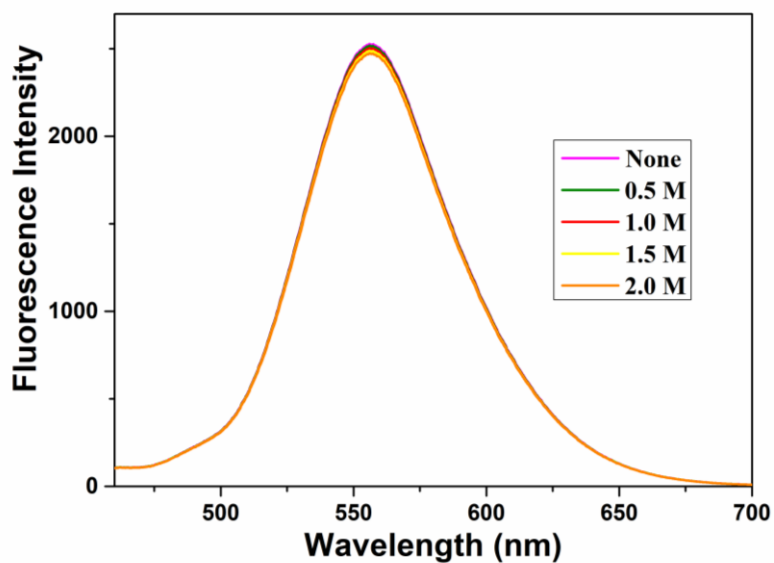


Fig.S14 The effect studies of the different ionic strengths (0.0-2.0 M KCl) on the fluorescence emission spectra of the N-CDs (0.04 mg/mL) at 420 nm excitation wavelength.

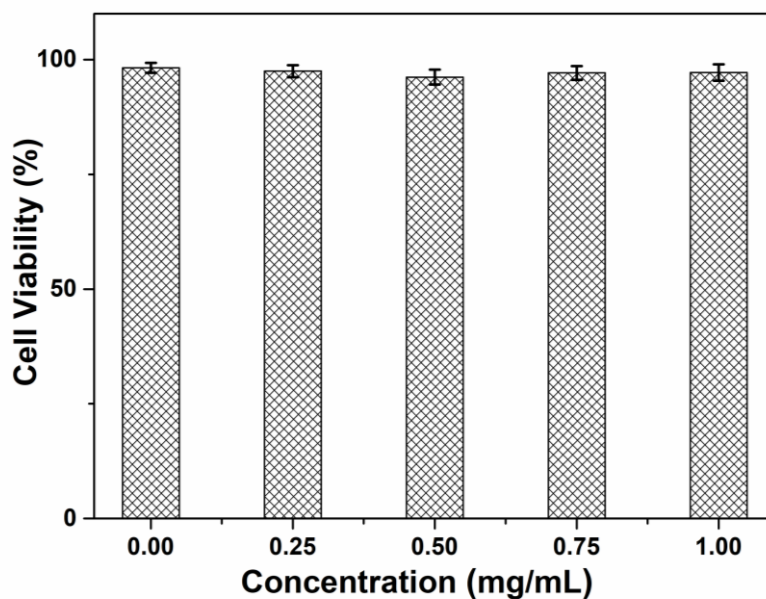


Fig.S15 Cytotoxic assays of the different concentrations of the N-CDs on HEp-2 Cells.

Table S1 Comparison between the reported carbon dots for Fe³⁺ sensing and the N-CDs

| Kinds of carbon dots | Ex/Em (nm) | Stokes shift | QYs | Detection limit (μM) | ref |
|-----------------------------|-------------------|---------------------|------------|-----------------------------|------------|
| N/P-CDs | 320/408 | 88 | 43.2 % | 0.33 μM | 3 |
| CDs | 360/442 | 82 | 8.64 % | 0.32 μM | 4 |
| N-CDs | 350/420 | 70 | 14 % | 0.9 μM | 5 |
| Si-CDs | 390/520 | 130 | 27.2 % | 13.7 nM | 6 |
| CDs | 340/426 | 86 | 10.5 % | 0.2 μM | 7 |
| N-CQDs | 360/440 | 80 | 23.48 % | 0.7462 μM | 8 |
| CDs | 360/436 | 76 | 6.2 % | 128 nM | 9 |
| CDs | 380/450 | 70 | 10.85 % | 9.55 μM | 10 |
| N-GQDs | 332/440 | 108 | 23.3 % | 90 nM | 11 |
| N-CDs | 330/420 | 90 | 13.6 % | 0.13 μM | 12 |
| N-CDs | 340/450 | 110 | 70 % | 107 nM | 13 |
| CDs | 360/450 | 90 | 9.8 % | 0.0154 μM | 14 |
| N-CDs | 355/442 | 87 | 27 % | 0.01 μM | 15 |
| N,Zn-CDs | 350/450 | 100 | 63.28 % | 0.027 μM | 16 |
| N,S-CDs | 360/443 | 83 | 28.9 % | 0.16 μM | 17 |
| F-CDs | 320/447 | 127 | 35.2 % | 10 nM | 18 |
| N-CDs | 360/438 | 78 | 54 % | 42nM | 19 |
| CQDs | 400/510 | 110 | 15 % | 50 nM | 20 |
| BNS-CDs | 500/600 | 100 | 5.44 % | 90 nM | 21 |
| N-CDs | 420/510 | 90 | 21.5 % | 0.18 μM | 22 |
| N-CDs | 450/556 | 106 | 20 % | 0.85 μM. | This work |

Table S2. Comparison between the organic dyes and the N-CDs

| Anion | E _x / E _m (nm) | Stokes shift | Detection limit (μM) | Ref. |
|--|--------------------------------------|--------------|----------------------|-----------|
| [H ₂ PO ₄] ⁻ | 365/495 | 131 | 0.176 | 23 |
| [H ₂ PO ₄] ⁻ | 365/401 | 36 | 0.046 | 24 |
| [H ₂ PO ₄] ⁻ | 330/535 | 205 | 0.0165 | 25 |
| [H ₂ PO ₄] ⁻ | 365/450 | 85 | 0.12 | 26 |
| [H ₂ PO ₄] ⁻ | 480/550 | 70 | 3.5 | 27 |
| [H ₂ PO ₄] ⁻ | 534/560 | 26 | 0.015 | 28 |
| [H ₂ PO ₄] ⁻ | 554/612 | 58 | 0.0169 | 29 |
| [HPO ₄] ²⁻ | 256/368 | 112 | 0.071 | 30 |
| [HPO ₄] ²⁻ | 460/496 | 36 | 0.025 | 31 |
| [HPO ₄] ²⁻ | 494/ 526 | 32 | 0.0621 | 32 |
| [HPO ₄] ²⁻ | 440/595 | 155 | 0.312 | 33 |
| [HPO ₄] ²⁻ | 450/556 | 106 | 0.80 | This work |

3. References

1. M. Zhang, Y. Gao, M. Li, M. Yu, F. Li, L. Li, M. Zhu, J. Zhang, T. Yi, C. Huang, *Tetrahedron Lett.* **2007**, *48*, 3709-3712.
2. Z. Qu, X. Zhou, L. Gu, R. Lan, D. Sun, D. Yu, G. Shi, *Chem. Commun.*, **2013**, *49*, 9830-9832.
3. J. Shangguan, J. Huang, D. He, X. He, K. Wang, R. Ye, X. Yang, T. Qing, J. Tang, *Anal. Chem.*, **2017**, *89*, 7477-7484.
4. J. Shen, S. Shang, X. Chen, D. Wang, Y. Cai, *Mater. Sci. Eng. C*, **2017**, *76*, 856-864.
5. R. Atchudana, T. N. J. I. Edison, K. R. Aseer, S. Perumalc, N. Karthika, Y. R. Lee, *Biosens. Bioelectron.*, **2018**, *99*, 303-311.
6. M. Shamsipur, K. Molaei, F. Molaabasi, M. Alipour, N. Alizadeh, S. Hosseinkhani, M. Hosseini, *Talanta*, **2018**, *183*, 122-130.
7. C. Sun, Y. Zhang, P. Wang, Y. Yang, Y. Wang, J. Xu, Y. Wang, W. W. Yu, *Nanoscale Res. Lett.*, **2016**, *11*, 110.
8. H. Qi, M. Teng, M. Liu, S. Liu, J. Li, H. Yu, C. Teng, Z. Huang, H. Liu, Q. Shao, A. Umar, T. Ding, Q. Gao, Z. Guo, *J. Colloid Interf. Sci.*, **2019**, *539*, 332-341.
9. S. Jayaweera, Y. Ke, X. Hu, W. J. Ng, *J. Photoch. Photobio. A*, **2019**, *370*, 156-163.

10. M. Zulfajri, G. Gedda, C. J. Chang, Y. P. Chang, G. G. Huang, *ACS Omega*, 2019, 4, 15382-15392.
11. J. Ju, W. Chen, *Biosens. Bioelectron.*, 2014, 58, 219-225.
12. W. Liu, H. Diao, H. Chang, H. Wang, T. Li, W. Wei, *Sensor. Actuat. B*, 2017, 241, 190-198.
13. L.J. Mohammed, K.M. Omer, *Sci. Rep.*, 2020, 10, 3028.
14. W. Zhang, L. Jia, X. Guo, R. Yang, Y. Zhang and Z. Zhao, *Analyst*, 2019, 144, 7421-7431.
15. Q. Huang, Q. Li, Y. Chen, L. Tong, X. Lin, J. Zhu, Q. Tong, *Sensor. Actuat. B*, 2018, 276, 82-88.
16. S. K. Tammina, D. Yang, X. Li, S. Koppala, Y. Yang, *Spectrochim. Acta A*, 2019, 222, 117141.
17. K. K. Chan, C. Yang, Y. H. Chien, N. Panwara and K. T. Yong, *New J. Chem.*, 2019, 43, 4734-4744.
18. D. Hong, X. Deng, J. Liang, J. Li, Y. Tao, K. Tan, *Microchem. J.*, 2019, 151, 104217.
19. L. Li, L. Shi, J. Jia, D. Chang, C. Dong, S. Shuang, *Analyst*, 2020, 145, 5450-5457.
20. K. M. Omer, D. I. Tofiq, A. Q. Hassan, *Mikrochim Acta*. 2018, 185, 466.
21. Y. Liu, W. Duan, W. Song, J. Liu, C. Ren, J. Wu, D. Liu, H. Chen, *ACS Appl. Mater. Interfaces*, 2017, 9, 12663-12672.
22. H. Deng, C. Tian, Z. Gao, S. W. Chen, Y. Li, Q. Zhang, R. Yu, and J. Wang, *Analyst*, 2020, 145, 4931-4936.
23. B. Turfan, E. U. *Org. Lett.*, 2002, 4, 2857-2859.
24. T. Mineno, T. Ueno, Y. Urano, H. Kojima, T. Nagano, *Org. Lett.*, 2006, 8, 5963-5966.
25. K. Du, J. Liu, R. Shen, P. Zhang, *Luminescence*, 2019, 34, 407-414.
26. C. Guo, S. Sun, Q. He, V. M. Lynch, J. L. Sessler, *Org. Lett.*, 2018, 20, 5414-5417.
27. L. He, R. P. Zuo, B. Wei, H. Tao, Q. Y. Cao, *Dyes. Pigments*, 2019, 168, 205-211.
28. J. Wu, X. Zhao, Y. Gao, J. Hu, Y. Ju, *Sensor. Actuat. B*, 2015, 221, 334-340.
29. S. Sen, M. Mukherjee, K. Chakrabarty, I. Hauli, S. K. Mukhopadhyay, P. Chattopadhyay, *Org. Biomol. Chem.*, 2013, 11, 1537-1544.
30. K. P. Wang, S. J. Zhang, C. D. Lv, H. S. Shang, Z. H. Jin, S. Chen, Q. Zhang, Y. B. Zhang, Z. Q. Hu, *Sensor. Actuat. B*, 2017, 27, 791-796.
31. T. Wei, G. Wu, B. Shi, Q. Lin, H. Yao, Y. Zhang, *Chin. J. Chem.*, 2014, 32, 1238-1244.

32. H. Tavallali, G. Deilamy-Rad, A. Moaddeli, K. Asghari, *Spectrochim. Acta A*, 2017, 183, 319-331.
33. M. R. Ganjalnia, M. Hosseini, Z. Memari, F. Faridbod, P. Norouzi, H. Goldooz, A. Badiei, *Anal. Chim. Acta*, 2011, 708, 107-110.